

Dynamic Modeling and Sensitivity Analysis of the Spherical Nanoparticle Topography using Piezoelectric Microcantilevers

R. Ghaderi*

Department of Mechanical Engineering,
Faculty of Technical and Engineering,
Shahrekord Branch, Islamic Azad University, Shahrekord, Iran
Email: Reza.Ghaderi@iaushk.ac.ir

*Corresponding author

Received: 6 September 2015, Revised: 14 December 2015, Accepted: 6 January 2016

Abstract: Piezoelectric microcantilevers (MCs) are a new generation of microbeams used in atomic force microscopes (AFMs). Due to their miniaturization of AFMs as well as their increased imaging precision and speed, these MCs are more popular than their classical counterparts. Given the widespread application of these beams in nanoparticle topography, analysis of their vibrating motion has attracted much attention in research circles. Exact vibrating analysis as well as study of the vibrating motion of these beams plays a key role in increasing their measuring accuracy in topography, and contributes to their optimum design. To this end, the nonlinear differential equation of vibrating motion of a MC was initially derived through Lagrange's method. Subsequently, the modal analysis and multiple time scale (MTS) methods were implemented to obtain an analytical solution to this equation. The effect on the nonlinear vibrational motion of the interaction between the nanoparticle and the probe was studied. The extended Fourier amplitude sensitivity test (eFAST) was conducted to analyze the nonlinearity sensitivity of the motion. The results obtained from this analysis made it possible to determine optimal geometric dimensions for the MC to increase its sensitivity to motion nonlinearity. Simulation results showed that, at higher inclined angles, the MC sensitivity to vibrational motion nonlinearity increased. The sensitivity analysis results revealed that the MC thickness and the length of its tip had the greatest effect on the MC sensitivity to the nonlinear force of interaction.

Keywords: Piezoelectric microcantilever, Sensitivity analysis, Spherical nanoparticle

References: Ghaderi, R, 'Dynamic Modeling and Sensitivity Analysis of the Spherical Nanoparticle Topography using Piezoelectric Microcantilevers', *Int J of Advanced Design and Manufacturing Technology*, Vol. 9/No. 1, 2016, pp. 73–82.

Biographical notes: **R. Ghaderi** received his PhD in Mechanical Engineering from University of IAU, Science and Research Branch in 2012. His current research interest includes Nonlinear Vibration and Micro-Electro-Mechanical Systems.

1 INTRODUCTION

Micro-Electro-Mechanical systems (MEMS) equipped with piezoelectric layers have been recently used in a wide range of micro-sensor and micro-actuator applications. This equipment utilize the direct and inverse effect of the piezoelectric material to create an actuator or a sensor [1-2]. MEMS equipped with piezoelectric layers are extensively used in resonators, micro-sensors, nanomanipulators, amplifiers, micro-pumps, and many other applications. In AFM, these microsystems can be used in nanorobots, biological cell manipulators, sensors, and surface imaging actuators [3-6]. These systems can create large displacements by applying a low voltage and can also be used to determine the displacements caused by external factors via measuring the output voltage. Many researchers [6-8] have studied the vibrating motion of the piezoelectric cantilevers at the macro scale.

In these studies, considering the cantilever application, the vibrating motion of the cantilever is simulated without taking into account the sample surface or the nanoparticle interaction force. Both linear and nonlinear vibrations have been studied in this regard. The studies conducted so far on piezoelectric MCs have often focused on the excitability and measurability of this type of MC [9-11]. Ito et al. [9] and Li et al. [10] utilized a MC equipped with a PZT piezoelectric layer as a self-actuator and self-sensor for sample surface topography. They used this MC in a scanning force microscope. They measured accurately the nanoscale sample surface topography without using the laser sensor.

Rogers et al. [12] used a piezoelectric MC with a ZnO layer in the AFM tapping mode. They were able to accurately obtain the topography of uneven surfaces at the nanoscale. Through their properly designed electric circuit and by applying the piezoelectric layer output voltage, they successfully conducted surface nanotopography with good accuracy, thus providing the possibility of operating piezoelectric microcantilevers in the self-measuring mode. Yuan et al. [13] manufactured a piezoelectric MC with a ZnO layer. Through investigating its actuation and measurement sensitivity, they found that ZnO was a suitable material for piezoelectric sensors and actuators. Piezoelectric MCs can not only determine surface topography with good accuracy, but also increase the imaging speed up to 5 times [14]. Few dynamic modeling studies have been conducted for analyzing the vibrating motion of the piezoelectric MCs as they interact with nanoparticles and sample surface. Liu et al. [15] statically analyzed a multi-layer piezoelectric MC. They presented a general model for static deformation of multi-layer and multi-segmented piezoelectric MCs. Wolf and Gottlieb [16] examined MC nonlinear vibrating motion without geometric discontinuities in the non-contact mode using the MTS analytic method. In this analysis, a uniform

piezoelectric layer was assumed across the MC so that the continuous beam model could be used for analyzing the vibrating motion. However, the MCs in use today contain geometric discontinuities due to the existence of the piezoelectric layer as well as their own tips. Under such conditions, the continuous beam model would not produce exact results in the analysis. Fung et al. [17] conducted a similar analysis using the finite element method for a piezoelectric MC with a triangular tip. They assumed the triangular tip as a concentrated mass at the end of the MC. The MC is dynamically simulated by neglecting the geometric discontinuities. Ghaderi and Nejat [18] studied the vibrating motion of piezoelectric MCs and their interaction with the sample surface using the nonlinear bending theory of beams. They provided efficient cantilever vibrating motion analysis only for the case where MC interacted with the specimen surface. For this reason, it was not possible in this analysis to simulate the vibrational behavior of the MC as it interacted with the nanoparticle during topography. Fairbairn and Moheimani [19] showed that the surface topography image resolution can be increased, and the vulnerability of the sample and the probe tip can be reduced by increasing the quality factor of piezoelectric MCs. McCarthy and Mahmoodi [20-21] obtained analytical expressions for the natural frequencies and mode shapes by solving the differential equation of motion. They also analyzed the MCs in the contact and tapping modes. This is a simplified analysis of a horizontal MC where geometric discontinuities are assumed negligible. The graphical method was used to examine the effects of different parameters on the vibrating motion. In this method, vibrating motion frequency and amplitude are studied by varying each parameter while keeping the other parameters constant. This method is used because it is simple, but it does not produce accurate results for analysis.

In this article, the nonlinear vibratory motion of a piezoelectric cantilever during its interaction with a nanoparticle was analytically modeled and simulated for the first time. To optimize the application of this type of cantilever in nanoparticle topography, we conducted the eFAST sensitivity analysis to determine the effect of MC geometric dimensions on its sensitivity to the nonlinearity of the interaction force.

2 DYNAMIC MODELING OF AFM PIEZOELECTRIC MC

The non-uniform MC was considered for dynamic modeling of the MC vibrating motion (Fig. 1). The inclined MC was fixed at one end. Its free end was exposed to the surface or the nanoparticle-probe tip interaction force. The MC vibrating excitation was done

by applying an alternating voltage to the piezoelectric layer.

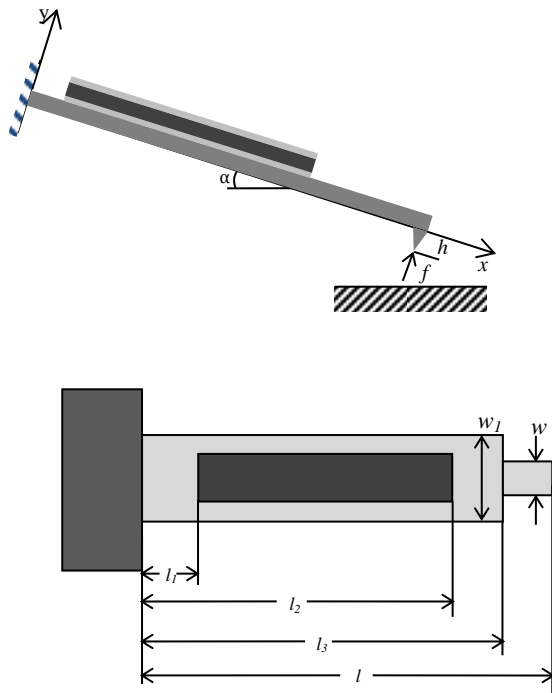


Fig. 1 Schematic of the piezoelectric MC, the coordinate system, and the loading applied

In the dynamic modeling of the MC, any relative displacement that might have occurred between the layers was disregarded. In view of the Euler-Bernoulli theory, the effects of shear deformation and rotational inertia on the motion were also neglected. The total kinetic energy of the MC can be expressed as follows:

$$KE = \frac{1}{2} \int_0^L \left\{ J(s) (\dot{v}^2 + 2\dot{v}^2 u' - 2v' \dot{u} \dot{v}' - 2\dot{v}^2 v'^2) + m(s) (\dot{u}^2 + \dot{v}^2) \right\} ds \quad (1)$$

where:

$$m(s) = \rho_1 b_1 w_1 (H_0 - H_{L_1}) + \sum_{i=1}^4 \rho_i b_i w_i (H_{L_i} - H_{L_{i+1}}) + \rho_1 b_1 w_1 (H_{L_2} - H_{L_3}) + \rho_1 b_1 w_1 (H_{L_3} - H_L) \quad (2)$$

$$J(s) = \frac{1}{12} \rho_1 w_1 b_1^3 (H_0 - H_{L_1}) + \frac{1}{12} \sum_{i=1}^4 \rho_i w_i b_i^3 (H_{L_i} - H_{L_{i+1}}) + \frac{1}{12} \rho_1 w_1 b_1^3 (H_{L_2} - H_{L_3}) + \frac{1}{12} \rho_1 w_1 b_1^3 (H_{L_3} - H_L) \quad (3)$$

$$H_{L_i} = H(s - L_i) ; H_{L_{i+1}} = H(s - L_{i+1}) \quad (4)$$

The potential energy of the piezoelectric MC during its bending (v) under an alternating voltage $P(t)$ can be expressed as follows:

$$U = \frac{1}{2} \int_0^L K(s) (v''^2 - 2v'' v'^2 - 2v' v'' u'' - 2v''^2 u') ds + \frac{1}{2} \int_0^L \gamma(s) (v'' - v'' u' - v' u'' - v'' v'^2) P(t) ds + \frac{1}{2} \int_0^L \xi(s) \left[u'^2 + u' v'^2 + \frac{1}{4} v'^4 \right] ds \quad (5)$$

where:

$$K(s) = K_1 (H_0 - H_{L_1}) + K_2 (H_{L_1} - H_{L_2}) + K_1 (H_{L_2} - H_{L_3}) + K_3 (H_{L_3} - H_L) \quad (6)$$

$$K_2 = \sum_{k=1}^4 E_k b_k w_k \left\{ \frac{\sum_{i=1}^4 E_i b_i w_i \left(\sum_{j=1}^i b_j - \frac{b_i}{2} \right)}{\sum_{i=1}^4 E_i b_i w_i} - \left(\sum_{j=1}^k b_j - \frac{b_k}{2} \right)^2 \times \frac{b_k^2}{12} \right\}; K_1 = E_1 \frac{w_1 b_1^3}{12}; K_3 = E_1 \frac{w_1 b_1^3}{12} \quad (7)$$

$$\gamma(s) = w_3 d_{31} E_3 \left[b_1 + b_2 + \frac{b_3}{2} - \sum_{i=1}^4 E_i b_i w_i \left(\sum_{j=1}^i b_j - \frac{b_i}{2} \right) / \sum_{i=1}^4 E_i b_i w_i \right] (H_0 - H_{L_1}) \quad (8)$$

Using Equations (1) and (5), the Lagrangian of the system can be expressed as follows:

$$L = \frac{1}{2} \int_0^L \left\{ J(s) (\dot{v}^2 + 2\dot{v}^2 u' - 2v' \dot{u} \dot{v}' - 2\dot{v}^2 v'^2) + m(s) (\dot{u}^2 + \dot{v}^2) - \xi(s) \left[u'^2 + u' v'^2 + \frac{1}{4} v'^4 \right] - K(s) (v''^2 - 2v'' v'^2 - 2v' v'' u'' - 2v''^2 u') - \psi(s) (v'' - v'' u' - v' u'' - v'' v'^2) P(t) \right\} ds \quad (9)$$

By applying the developed Hamilton principle, the differential equation governing the piezoelectric MC interacting with the nanoparticle can be written as:

$$m(s) \ddot{v} + (K(s) v'')'' + [v'(K(s) v' v'')]'' + \left\{ v' \int_L^s m(s) \left[\int_0^s (\dot{v}' v' + \dot{v}^2) dx \right] ds \right\}' - \left[\frac{1}{2} v' [\psi(s) v' P(t)] \right]' + \left[\frac{1}{4} \psi(s) v'^2 P(t) \right]'' - \left[\frac{1}{2} \psi(s) P(t) \right]'' = f \sin \theta \delta(s - L) \quad (10)$$

In the above differential equation of motion, f is the interaction force between the MC tip and the nanoparticle. The effect of the nanoparticle on the vibrating motion of MC can be extracted using the van der Waals force formulation obtained via finding the continuum mechanics solution for the interaction between the MC tip and the spherical particle. That is [3]:

$$f(R) = -\frac{2}{3} \frac{HR_p R_t}{(R + R_t + R_p)^2 (R - R_t - R_p)^2} \quad (11)$$

where R_t and R_p are the radii of the tip and the nanoparticle respectively. H is the Hamaker constant, and R is the distance between the MC tip and the nanoparticle at any given moment, obtained as:

$$R = \sqrt{[d_0 + u(L, t)]^2 + v^2(L, t)} \quad (12)$$

In this equation, d_0 is the equilibrium distance between the MC tip and the nanoparticle when the tip is above the nanoparticle. In order to solve the differential equation of motion (equation 10), the MC can be divided into four homogeneous cantilevers and the continuity condition applied at each stage. Using the Galerkin linear approximation, the MC deformation can be expressed as [16]:

$$v(s, t) = \sum_{i=1}^{\infty} \alpha_n(s) q_n(t) \quad (13)$$

where $q_n(t)$ is the global coordinate, and $\alpha_n(s)$ is comparison function of the n -th vibrating mode. Since the MC is divided into four homogeneous beams, the comparison function can be written as:

$$\alpha_n(s) = \begin{cases} A_n^{(1)} \sin \varphi_n^{(1)} s + B_n^{(1)} \cos \varphi_n^{(1)} s + C_n^{(1)} \sinh \varphi_n^{(1)} s \\ + D_n^{(1)} \cosh \varphi_n^{(1)} s, & 0 \leq s \leq L_1 \\ A_n^{(2)} \sin \varphi_n^{(2)} s + B_n^{(2)} \cos \varphi_n^{(2)} s + C_n^{(2)} \sinh \varphi_n^{(2)} s \\ + D_n^{(2)} \cosh \varphi_n^{(2)} s, & L_1 \leq s \leq L_2 \\ A_n^{(3)} \sin \varphi_n^{(3)} s + B_n^{(3)} \cos \varphi_n^{(3)} s + C_n^{(3)} \sinh \varphi_n^{(3)} s \\ + D_n^{(3)} \cosh \varphi_n^{(3)} s, & L_2 \leq s \leq L_3 \\ A_n^{(4)} \sin \varphi_n^{(4)} s + B_n^{(4)} \cos \varphi_n^{(4)} s + C_n^{(4)} \sinh \varphi_n^{(4)} s \\ + D_n^{(4)} \cosh \varphi_n^{(4)} s, & L_3 \leq s \leq L \end{cases} \quad (14)$$

where $\varphi_n^{(r)} = \omega_n^{(r)} m^{(r)} / K^{(r)}$ and the $A_n^{(r)}$, $B_n^{(r)}$, $C_n^{(r)}$ and $D_n^{(r)}$ coefficients are unknown values that can be calculated using the boundary conditions, applying the principle of continuity for deformation, slope, bending moment, and shear force, and normalizing with respect to mass:

$$\int_0^L m(s) \alpha_n^2(s) dx = 1 \quad (15)$$

By substituting the equations (13) and (14) into the differential equation of motion (equation 10) and through inner multiplication of both sides of the equality by $\alpha_n(s)$, and integrating along the MC length, the ordinary differential equation motion can be written as:

$$\ddot{q}_n + \mu_n \dot{q}_n + \omega_n^2 q_n + \tau_{n1} q_n^2 + \tau_{n2} q_n^3 + \tau_{n3} (q_n^2 \ddot{q}_n + q_n \dot{q}_n^2) \\ + \tau_{n4} q_n^2 P(t) + \tau_{n5} P(t) + \tau_{n6} = 0 \quad (16)$$

where:

$$\omega_n = \int_0^L \alpha_n(s) \left\{ \frac{d^2}{ds^2} \left[K(s) \frac{d^2 \alpha_n(s)}{ds^2} \right] \right. \\ \left. + f' \sin \theta \alpha_n(s) \delta(s-L) \right\} ds \quad (17)$$

$$\tau_{n1} = \int_0^L 0.5 \alpha_n^3(s) f'' \sin \theta \delta(s-L) dx \quad (18)$$

$$\tau_{n2} = \int_0^L \alpha_n(s) \frac{d}{ds} \left[\frac{d \alpha_n}{ds} \frac{d}{ds} \left(K(s) \frac{d \alpha_n}{ds} \frac{d^2 \alpha_n}{ds^2} \right) \right. \\ \left. + \frac{f''' \sin \theta}{6} \alpha_n^3(s) \delta(s-L) \right] ds \quad (19)$$

$$\tau_{n3} = \int_0^L \alpha_n(s) \frac{d}{ds} \left[m(s) \frac{d \alpha_n}{ds} \int_L^s 2 \left(\frac{d \alpha_n}{ds} \right)^2 ds ds \right] ds \quad (20)$$

$$\tau_{n4} = \frac{1}{4} \int_0^L \alpha_n(s) \frac{d^2}{ds^2} \left[\psi(s) \left(\frac{d^2 \alpha_n}{ds^2} \right)^2 \right] ds \\ - \frac{1}{2} \int_0^L \alpha_n(s) \frac{d^2}{ds^2} \left[\frac{d \alpha_n}{ds} \frac{d^2}{ds^2} \left(\psi(s) \frac{d \alpha_n}{ds} \right) \right] ds \quad (21)$$

$$\tau_{n5} = - \int_0^L \alpha_n(s) \frac{d^2 \psi(s)}{ds^2} ds \quad (22)$$

$$\tau_{n6} = - \int_0^L \alpha_n(s) f(d_0) \sin \theta ds \quad (23)$$

3 FREQUENCY RESPONSE ANALYSIS

The analytic MTS method can be used to obtain the frequency response of the MC motion near the nanoparticle. This method is used to solve the differential equation (16). The time parameter can be expanded into the following form:

$$q_n(t) = \varepsilon q_{n1}(T_0, T_1, T_2) + \varepsilon^2 q_{n2}(T_0, T_1, T_2) \\ + \varepsilon^3 q_{n3}(T_0, T_1, T_2) + o(\varepsilon^4) \quad (24)$$

where $T_n = \varepsilon^n t$, ε is a parameter much smaller than one.

The time derivatives can be expressed as follows:

$$\frac{d}{dt} = D_0 + \varepsilon D_1 + \varepsilon^2 D_2 + o(\varepsilon^3) \quad (25)$$

where $D_n = \partial / \partial T_n$. To solve the ordinary differential equation of motion (16), the excitation voltage and the linear damping were scaled to the same order as the perturbation problem. In other words:

$$P(t) = \varepsilon^3 P(t); \mu_n = \varepsilon^2 \mu_n \quad (26)$$

By substituting equations (24)-(26) into equation (16) and separating the power coefficients of ε , we can write:

$$O(\varepsilon): D_0^2 q_{n1} + \omega_n^2 q_{n1} = 0 \quad (27)$$

$$O(\varepsilon^2) : D_0^2 q_{n2} + \omega_n^2 q_{n2} + 2D_0 D_1 q_{n1} + \tau_{n1} q_{n1}^2 = 0 \quad (28)$$

$$O(\varepsilon^3) : D_0^2 q_{n3} + \omega_n^2 q_{n3} + \mu_n D_0 q_{n1} + 2D_0 D_2 q_{n1} + 2D_0 D_1 q_{n2} + D_1^2 q_{n1} + 2\tau_{n1} q_{n1} q_{n2} + \tau_{n4} q_{n1}^2 P(T_0) + \tau_{n2} q_{n1}^3 + \tau_{n3} [D_0^2 q_{n1} + (D_0 q_{n1})^2] + \tau_{n5} P(T_0) + \tau_{n6} = 0 \quad (29)$$

The solution of the linear differential equation (27) can be expressed as:

$$q_{n1} = B_n(T_1, T_2) e^{i\omega_n T_0} + B_n^*(T_1, T_2) e^{-i\omega_n T_0} \quad (30)$$

where B_n is the complex parameter, and B_n^* is its complex conjugate. By substituting equation (30) into equation (28), we have:

$$D_0^2 q_{n2} + \omega_n^2 q_{n2} - \tau_{n1} (B_n^2 e^{2i\omega_n T_0} + B_n B_n^*) + 2i\omega_n D_1 B_n e^{i\omega_n T_0} + cc = 0 \quad (31)$$

Since the steady state solution of the differential equation must be obtained, the singular terms in equation (31) are neglected. In other words, the terms containing the term $e^{i\omega_n T_0}$ are disregarded. Thus, we obtain $D_1 B_1 = 0$, or, $B_1 = B_1(T_2)$, and:

$$q_{n2} = \frac{-\tau_{n1} B_n^2}{3\omega_n^2} e^{2i\omega_n T_0} + 2 \frac{B_n B_n^*}{\omega_n^2} + cc \quad (32)$$

In AFM applications, the MC is excited through a frequency close to its resonant frequency. The resonant frequency, Ω , can be expressed as:

$$\Omega = \omega_n + \varepsilon^2 \sigma \quad (33)$$

where σ is the detuning parameter indicating the deviation from the natural frequency. If the excitation voltage is defined as $P = P e^{i\Omega t}$, Equation (29) can be expressed as follows after removing the singular terms and substituting into equation (32):

$$2i\omega_n D_2 B_n + [3\tau_{n2} - (10/3)\tau_{n1}^2 - 2\omega_n^2 \tau_{n3}] B_n^2 B_n^* + \frac{P}{2} e^{i\sigma\omega_n T_2} (\tau_{n4} B_n B_n^* - \tau_{n5}) + i\mu_n \omega_n B_n + \frac{P}{2} \tau_{n4} B_n^2 e^{-i\sigma\omega_n T_2} = 0 \quad (34)$$

To solve the equation (34), B_n should be expressed in polar coordinates as:

$$B_n = \frac{1}{2} b_n e^{i\beta_n}; \quad B_n^* = \frac{1}{2} b_n e^{-i\beta_n} \quad (35)$$

where b_n and β_n are the real amplitude values and the response phase respectively. By substituting the values in (35) in the equation (34) and separating the real and imaginary parts, we can write:

$$\begin{cases} \frac{3\tau_{n2} - (10/3)\tau_{n1}^2 - 2\omega_n^2 \tau_{n3}}{8} b_n^3 + \omega_n b_n \dot{\xi}_n \\ + 1/2 (\tau_{n5} - 1/2 \tau_{n4} b_n^2) \cos \xi_n - \sigma \omega_n^2 b_n = 0 \\ 2\omega_n \dot{b}_n + \mu_n \omega_n b_n + \tau_{n5} P \sin \xi_n = 0 \end{cases} \quad (36)$$

where $\xi_n = \sigma T_2 - \beta_n$. Equation (36) expresses the amplitude response modulation (b_n) and the phase response (ξ_n). Since the steady-state response is required here, \dot{b}_n and $\dot{\xi}_n$ are assumed to be zero. By quadrating and adding the two omitted ξ_n terms, the nonlinear equation of frequency response is obtained as follows:

$$\left(\tau_{n5} \frac{(3\gamma_{n2} - (10/3)\gamma_{n1}^2 - 2\omega_n^2 \gamma_{n3}) b_n^3 - 8\omega_n^2 \sigma b_n}{16\tau_{n5} - 8\tau_{n4} b_n^2} \right)^2 + (1/2 \mu_n \omega_n a_n)^2 = (1/2 \tau_{n5} P)^2 \quad (37)$$

The obtained frequency response function shows that for some values of the detuning parameter, more than one amplitude is obtained. This is referred to as the frequency response softening.

4 NUMERICAL SIMULATION AND RESULTS

A silicon MC was assumed in the numerical simulation of the piezoelectric MC vibrating motion near a spherical nanoparticle. A layer of piezoelectric ZnO was included on the base layer. The piezoelectric layer was enclosed between two Ti/Au electrodes. The geometrical specifications and physical properties of the MC are given in tables (1) and (2) respectively. The Lennard-Jones model coefficients were selected as $\sigma = 0.34$ (nm) and $H = 10^{18}$ (J) based on Ref. [16].

Table 1. Specifications of the piezoelectric MC material [11]

	Material	E (Gpa)	ρ (Kg/m ³)
Base Layer	Si	105	2330
Lower Electrode	Ti/Au	78	19300
Piezoelectric Layer	Zno	104	6390
Upper Electrode	Ti/Au	78	19300
tip	Si	105	2330

Wolf and Gottlieb [16] studied a piezoelectric MC with a uniform cross section and a piezoelectric layer covering the entire length in interaction with sample surface. In extracting the differential equation of motion, the actuator moment of the piezoelectric layer and the interaction force was imposed as the cantilever boundary conditions. Here, the MC was considered uniform with an overall PZT-5H piezoelectric layer to allow for the comparison between our results and those obtained by Wolf and Gottlieb. Fig. 2 shows the MC frequency response in the two equilibrium distances (d) of 1 and 2 nm. Results indicate

that there is good agreement between the two solution methods.

According to the Van der Waals force model, the interaction force between the probe tip and the sample surface depends on the distance between the tip and the nanoparticle or the sample surface. A reduced distance increases the nonlinear force, and consequently, increases the nonlinearity of the vibrating motion. An increased nonlinearity of the vibrating motion decreases the resonant frequency of the MC vibrating motion. In the frequency response curve, the reduction in the resonant frequency appears as a curvature in the curve.

Obviously, larger nonlinearity intensifies the curvature of the curve or the softening phenomenon. Fig. 3 shows the increased softening of the frequency response when the MC approaches the nanoparticle or the sample surface. The curves also show that the curvature of the frequency response curve is larger when the MC interacts with the sample surface compared to the nanoparticle.

Table 2. The geometrical specifications of the simulated MC [11]

	h (μm)	W (μm)	L (μm)
Base Layer	4	250	375
Lower Electrode	0.25	130	330
Piezoelectric Layer	4	130	330
Upper Electrode	0.25	130	330
tip	15	55	125

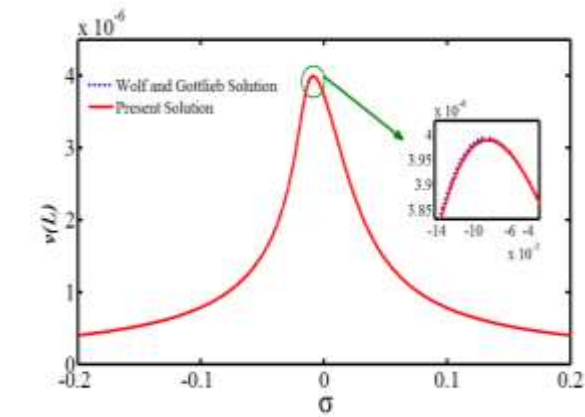
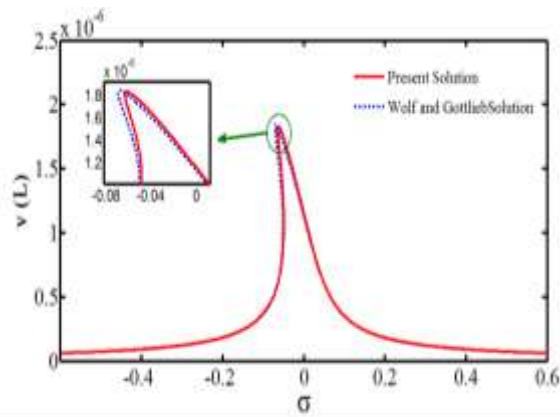


Fig. 2 The frequency response of piezoelectric MC near the sample surface

This is very important in the nanoparticle topography in the AFM frequency mode. In the frequency mode, the reduced resonant frequency when the MC tip approaches the nanoparticle can be used for the localization of nanoparticles on the surface.

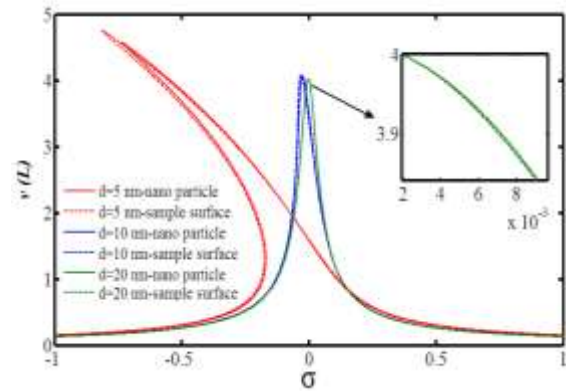


Fig. 3 The MC frequency response near the sample surface and nanoparticle

Another factor that influences the intensification of the interaction force of the sample surface or nanoparticle is the Hamaker constant. According to Eq. (11), an increased Hamaker constant increases the nonlinear interaction force. An increased force, and hence an intensified nonlinear factor, increases the curvature of the frequency response curve. The increased curvature can be seen in Fig. 4.

This is very important in the nanoparticle topography in the AFM frequency mode. In the frequency mode, the reduced resonant frequency when the MC tip approaches the nanoparticle can be used for the localization of nanoparticles on the surface.

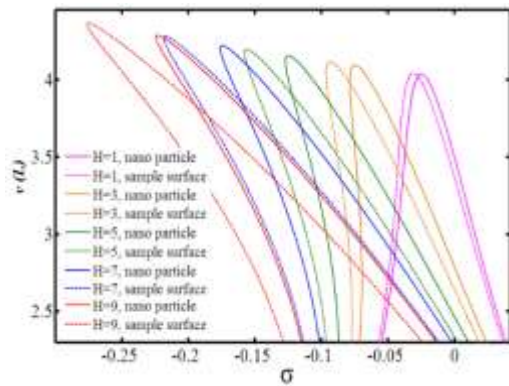


Fig. 4 Effect of the Hamaker constant on the MC frequency response

Since installing the MC horizontally is difficult in practically, it is essential to study the vibrating behavior of the inclined angle near the sample surface and nanoparticle. This study determines the effect of inclined angle on the vibrating motion. It also helps to obtain the optimum installation angle.

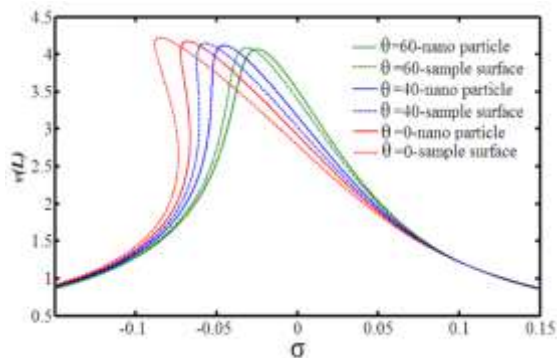


Fig. 5 Effect of the inclined angle on the MC frequency response

Fig. 5 shows the effect of inclined angle on the frequency response of the vibrating motion. Results show that vibrating motion sensitivity to the interaction force between nanoparticle and sample surface decreases by increasing the inclined angle. This can be attributed to the reduced component of the force effective on the vibrating motion as a result of increasing the MC angle. Therefore, to increase the MC sensitivity to interaction forces, and thereby, to increase the accuracy of the nanoparticle and sample surface topography, it is recommended to install the MC at a slight horizontal angle. This figure also shows that the frequency response sensitivity to angle is higher in the interaction with the sample surface compared to the nanoparticle.

4-1 THE EFFECT OF MC GEOMETRY ON THE FREQUENCY RESPONSE

The nonlinear interaction force between the probe tip and the sample surface or nanoparticle results in the nonlinear

vibration behavior of the MC. According to the MTS analysis, the intensity of the vibrating motion nonlinearity can be introduced by the coefficient which accounts for the curvature of frequency response curve. The nonlinear coefficient γ can be used as an indicator to determine the system nonlinearity. This coefficient depends not only on the force between the tip and the nanoparticle but also on the geometry. Therefore, the effect of MC geometry on the coefficient γ was studied to optimize the geometrical dimensions.

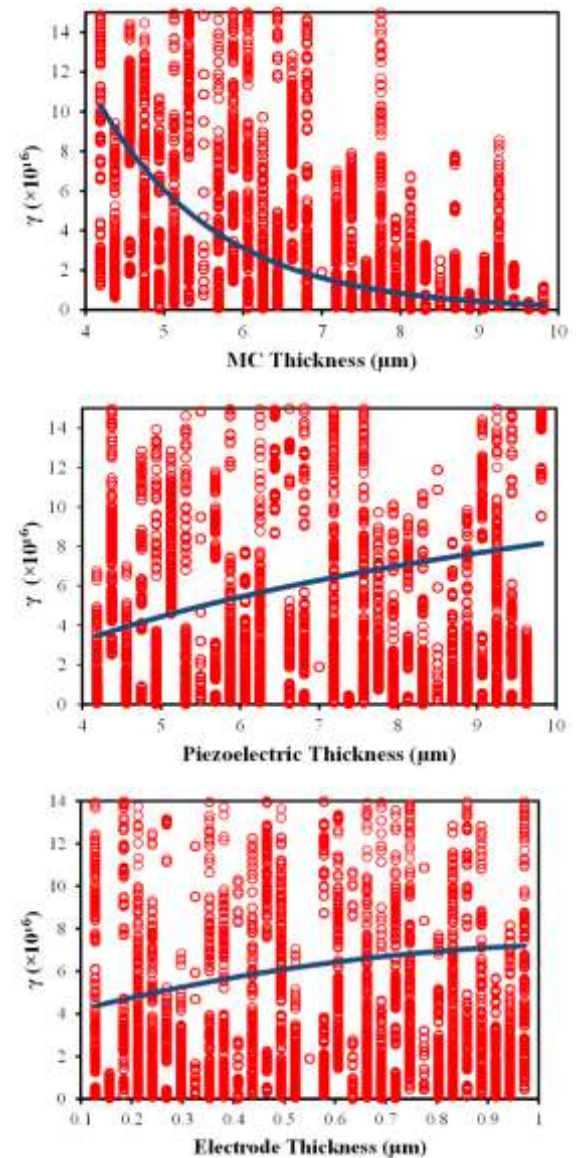


Fig. 6 Effect of thickness of the MC layers on γ

The aim of optimization is to obtain the best geometrical dimensions to increase the MC sensitivity to the nanoparticle interaction force.

Sensitivity analysis was performed based on statistical methods to study the effect of geometrical dimensions on the coefficient γ . The eFAST method is very effective in

analyzing nonlinear models, absolute sensitivity analysis of the inputs, and determination of the system output sensitivity to input variables [22]. Therefore, the eFAST method was used to analyze the sensitivity of the MC vibrating motion. This method simulates the inputs based on the probability distributions using ANOVA. ANOVA can be used to investigate the interaction between multiple inputs on the outputs. The sensitivity of the model output for one or more inputs can be then evaluated. Fig. 6 shows the effect of the thickness of each MC layer on the coefficient γ . As can be seen, by increasing the thickness of the main MC layer, it decreases the coefficient γ . This reduction indicates the reduced MC sensitivity to the nonlinearity of the nanoparticle interaction force. Unlike the main layer thickness, increasing the thickness of the piezoelectric layer and the electrodes increases the MC sensitivity to the force nonlinearity. Therefore, it can be concluded that, in order to increase the MC sensitivity, the thickness of the main layer must be selected as low as possible, whereas the other layers must be selected as thick as possible.

Fig. 7 shows that the tip width does not considerably affect the MC sensitivity to the nonlinear force. Fig. 8 shows that an increased MC length reduces the MC sensitivity to the nonlinearity of the vibrating motion. Results show that, compared to other layer lengths, this geometric parameter has a lower effect on the coefficient γ . Unlike the MC length, the length of the piezoelectric layer and the tip considerably affect γ . Therefore, they should be considered as important parameters in the piezoelectric MC design in AFM applications. Fig. 7 shows that the tip width does not considerably affect the MC sensitivity to the nonlinear force.

Fig. 8 shows that an increased MC length reduces the MC sensitivity to the nonlinearity of the vibrating motion. Results show that, compared to other layer lengths, this geometric parameter has a lower effect on the coefficient γ . Unlike the MC length, the length of the piezoelectric layer and the tip considerably affect γ . Therefore, they should be considered as important parameters in the piezoelectric MC design in AFM applications.

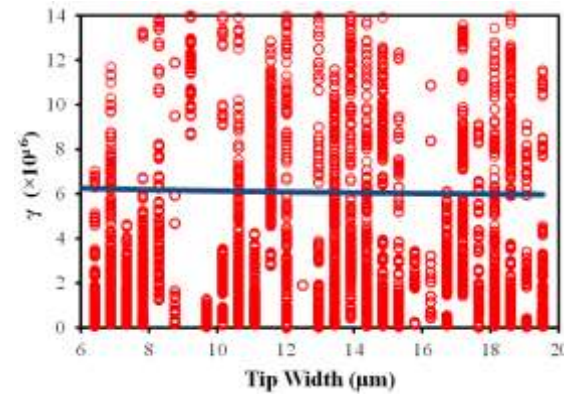
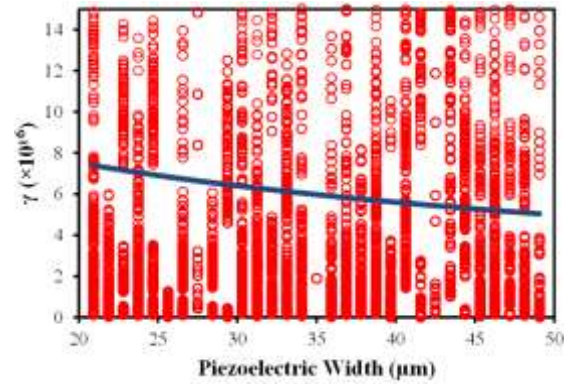
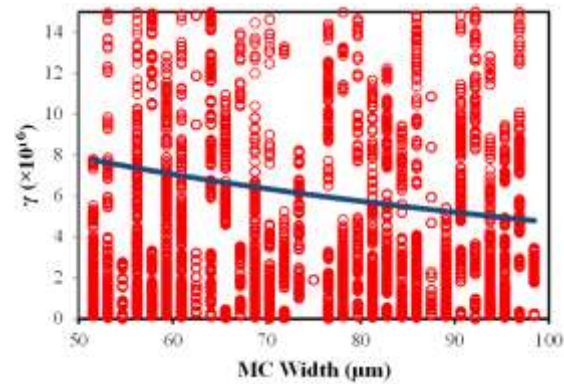
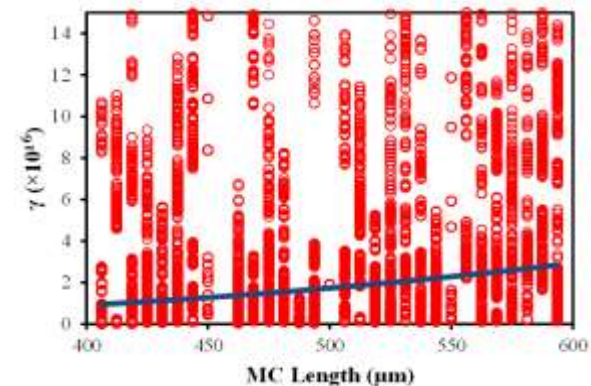


Fig. 7 Effect of width of the MC layers on γ



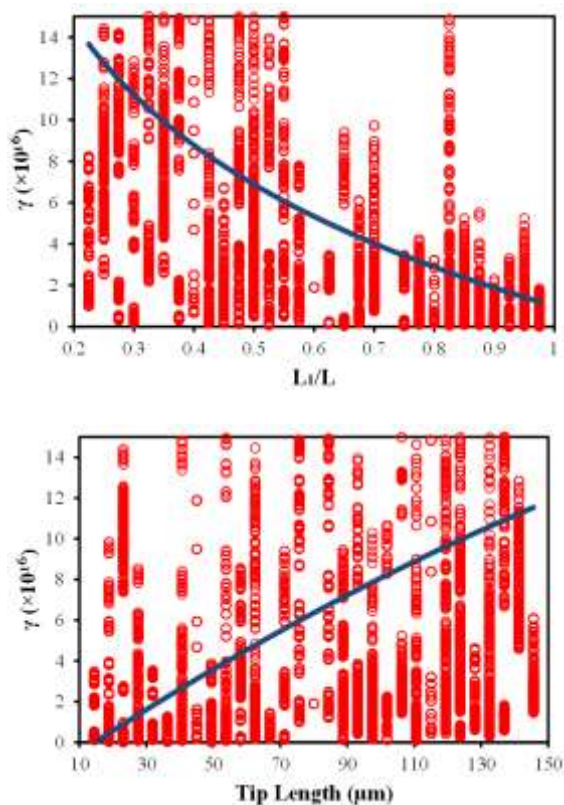


Fig. 8 Effect of length of the MC layers on γ

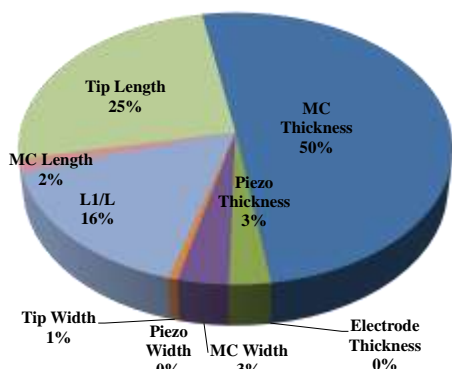


Fig. 9 Sensitivity of the coefficient γ to MC geometrical dimensions

Fig. 9 shows the sensitivity of the nonlinear coefficient γ to each geometrical dimension of the piezoelectric MC. As can be seen, the thickness of the MC main layer, the tip length, and the piezoelectric layer length have the most influence on coefficient γ , whereas the width of the layers had the minimal effect on the coefficient γ . Therefore, in the design and manufacture of piezoelectric MCs in the AFM applications, in order to maximize the sensitivity of AFM to the nonlinear nanoparticle interaction force, it is recommended to focus on the geometric parameters of the thickness of the MC main layer, the tip length, and the piezoelectric layer length. This way, the optimum geometrical dimensions in the AFM applications can be

obtained by minimal changes possible in the MC geometry.

5 CONCLUSION

The flexural vibrating motion of piezoelectric MC subjected the nonlinear force of the nanoparticle and sample surface was investigated here. The governing differential equation was solved using the non-uniform beam model and the MTS method and the frequency response of nonlinear vibrating motion was extracted. The eFAST method was employed for sensitivity analysis to determine the effect of the MC geometrical dimensions on the vibrating motion nonlinearity. The results of the motion simulation and sensitivity analysis are as follows:

1. The vibrating motion of the MC piezoelectric near the nanoparticle and the sample surface led to the softening of the frequency response curve. This softening was intensified by reducing the equilibrium distance. The simulation results also showed that, compared to the nanoparticle, the curvature of the curve was higher in the presence of interaction with the sample surface.
2. By increasing the Hamaker constant, the curvature of the frequency response curve in the MC interaction with nanoparticle and sample surface increased. An increased MC angle decreased the effect of force on the vibrating motion, and consequently, reduced the MC sensitivity to the interaction force nonlinearity.
3. The sensitivity analysis results showed that the thickness of the MC, the tip length, and the piezoelectric layer length were the most influential geometric parameters on the non-linearity of the vibrating motion. The width of the layers and the MC length had the least effect on the motion non-linearity.
4. The results of the sensitivity analysis showed that increasing the MC thickness and the tip length reduced the MC sensitivity to the nanoparticle and probe interaction force. Therefore, to optimally design this type of MCs and to increase topography accuracy, the MC width must be as small as possible and the tip as long as possible.
5. The larger the ratio of the piezoelectric layer length to the MC length, the higher the MC sensitivity to the interaction force nonlinearity. Therefore, the use of a MC with an overall piezoelectric layer can increase the accuracy of the topographic images obtained from the nanoparticles.

REFERENCES

[1] Dong, W., Lu, X., Cui, Y., Wang, J., and Liu, M., "Fabrication and characterization of microcantilever

- integrated with PZT thin film sensor and actuator," *Thin Solid Films*, Vol. 515, 2007, pp. 8544-8548.
- [2] Yamashita, K., Yang, Y., Nishimoto, T., Furukawa, K., and Noda, M., "Piezoelectric vibratory-cantilever force sensors and axial sensitivity analysis for individual triaxial tactile sensing," *Sensors Journal*, Vol. 13, No. 3, 2011, pp. 1074-1080.
- [3] Jalili, N., and Laxminarayana, K., "A review of atomic force microscopy imaging systems application to molecular metrology and biological sciences," *International Journal of Mechanics*, Vol. 14, No. 8, 2004, pp. 907-945.
- [4] Korayem, M. H., and Zakeri, M., "Sensitivity analysis of nanoparticles pushing critical conditions in 2-D controlled nanomanipulation based on AFM," *International Journal of Advances Manufacturing and Technology*, Vol. 41, 2009, pp. 714-725.
- [5] Adams, J. D., Parrott, G., Bauer, C., Sant, T., Manning, L., Jones, M., Rogers, B., McCorkle, D., and Ferrel T. L., "Nanowatt chemical vapor detection with a self-sensing, piezoelectric microcantilever array," *Applied Physics Letters*, Vol. 83, 2003, pp. 3428-3236.
- [6] Korayem, M. H., Esmailzadehha, S., Rahmani, N., and Shahkarami, M., "Nano manipulation with rectangular cantilever of atomic force microscope (AFM) in a virtual reality environment," *Digest Journal of Nanoscience and Biomaterial*, Vol. 7, No. 2, 2012, pp. 435-445.
- [7] Bashash, S., Saeidpourazar, R., and Jalili, N., "Development, analysis and control of a high-speed laser-free atomic force microscope," *Review of Scientific Instruments*, Vol. 81, 2010, pp. 78-84.
- [8] Saeidpourazar, R., and Jalili, N., "Towards fused vision and force robust feedback control of nanorobotic-based manipulation and grasping," *Mechatronics*, Vol. 18, 2008, pp. 566-577.
- [9] Itoh, T., and Suga, T., "Self-excited force sensing microcantilevers with piezoelectric thin films for dynamic scanning force microscopy," *The 8th Int. Conference on Solid Sensors and Actuators*, Stockholm, 1995, pp. 87-91.
- [10] Lee, C., Itoh, T., and Suga, T., "Self-excited piezoelectric PZT microcantilevers for dynamic SFM-with inherent sensing and actuating capabilities," *Sensors and Actuators A*, Vol. 72, 1999, pp. 179-187.
- [11] Mahmoodi, S. N., Dagag, M. F., and Jalili, N., "On the nonlinear-flexural response of piezoelectrically driven microcantilever sensors," *Sensors and Actuators A*, Vol. 153, 2009, pp. 171-179.
- [12] Rogers, B., Manning, L., Sulchek, T., and Adams, J. D., "Improving tapping mode atomic force microscopy with piezoelectric cantilevers," *Ultramicroscopy*, Vol. 100, 2004, pp. 267-276.
- [13] Yuan, Y., Chow, K. Sh, Du, H., Wang, P., Zhang, M., Yu, Sh., and Liu, B., "A ZnO thin-film driven microcantilever for nanoscale actuation and sensing," *International Journal of Smart and Nanomaterials*, Vol. 4, No. 2, 2012, pp.128-141.
- [14] Acosta, C. J., Polesel-Maris, J., Thoyer, F., Xie, H., Haliyo, S., and Régnier, S., "Gentle and fast atomic force microscopy with a piezoelectric scanning probe for nanorobotics applications," *Nanotechnology*, Vol. 24, No. 6, 2013, 065502.
- [15] Liu, M. W., Tong, J. H., Wang, J., Dong, W. J., Cui, T. H., and Wang, L. D., "Theoretical analysis of the sensing and actuating effects of piezoelectric multimorph cantilevers," *Microsystem Technology*, Vol. 12, 2006, pp. 335-342.
- [16] Wolf, K., and Gottlieb, O., "Nonlinear dynamics of a noncontacting atomic force microscope cantilever actuated by a piezoelectric layer," *Journal of Applied Physics*, Vol. 91, No. 7, 2002, pp. 4701-4709.
- [17] Fung, R. F, and Huang, S. C, "Dynamic modeling and vibration analysis of the atomic force microscope", *ASME Journal of Vibration and Acoustic*, Vol. 123, 2001, pp. 502-509.
- [18] Ghaderi, R., and Nejat, A., "Nonlinear mathematical modeling of vibrating motion of nanomechanical cantilever active probe," *Latin American Journal of Solids and Structures*, Vol. 11, 2014, pp. 369-385.
- [19] Fairbairn, M., and Moheimani, S. O. R, "Sensorless enhancement of an atomic microscope micro-cantilever quality factor using piezoelectric shunt control," *Review of Scientific Instruments*, Vol. 84, 2013, 053706.
- [20] McCarty, R., and Mahmoodi, S. N., "Nonlinear forced response of piezoelectric microcantilevers with application to tapping mode atomic force microscopy," *Proceeding SPIE 9057, Active and Passive Smart Structures and Integrated Systems*, 2014, 905722.
- [21] McCarty, R., and Mahmoodi, S. N., "Parameter sensitivity analysis of nonlinear piezoelectric probe in tapping mode atomic force microscopy for measurement improvement," *Journal of Applied Physics*, Vol. 115, No. 7, 2014, 074501-074501-9.
- [22] Dinkelbach, W., "Sensitivity analysis and parametric programming," *Springer- Verlag*, New York, 1969, Chap. 5.